

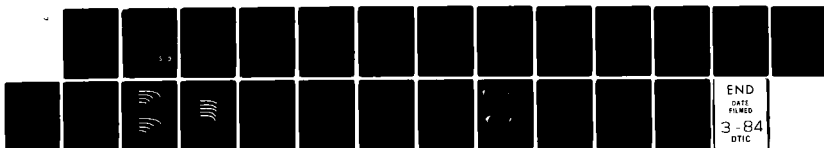
AD-A137 840

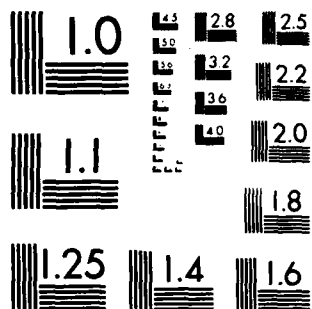
BENDING OF BEAMS SUBJECTED TO TRANSVERSE IMPACTS(U)  
MATERIALS RESEARCH LABS ASCOT VALE (AUSTRALIA)  
R L WOODWARD APR 83 MRL-R-886

1/1

UNCLASSIFIED

F/G 20/11 NL





MICROCOPY RESOLUTION TEST CHART  
NATIONAL BUREAU OF STANDARDS-1963-A



AD A137840

**DEPARTMENT OF DEFENCE**  
**DEFENCE SCIENCE AND TECHNOLOGY ORGANISATION**  
**MATERIALS RESEARCH LABORATORIES**  
**MELBOURNE, VICTORIA**

**REPORT**  
**MRL-R-886**

BENDING OF BEAMS SUBJECTED TO TRANSVERSE IMPACTS

R.L. Woodward

THE UNITED STATES NATIONAL  
TECHNICAL INFORMATION SERVICE  
IS AUTHORIZED TO  
REPRODUCE AND SELL THIS REPORT

Approved for Public Release

**DTIC**  
**ELECTE**  
**S** **D**  
FEB 14 1984  
**E**

FILE COPY



**C** Commonwealth of Australia  
APRIL, 1983

**DEPARTMENT OF DEFENCE  
MATERIALS RESEARCH LABORATORIES**

**REPORT  
MRL-R-886**

**BENDING OF BEAMS SUBJECTED TO TRANSVERSE IMPACTS**

R.L. Woodward

**ABSTRACT**

Transverse projectile impacts on the ends of free-free beams of circular cross section produced evidence of hinges in the beams and strain distributions which could be used for comparisons with a rigid-plastic approach to the dynamic response of structures and for comparisons with a finite element computer code solution. The rigid-plastic approach describes the mechanism of bending and hinge development and motion correctly but the simplifications inherent in the model prevent it from accurately predicting the detail. The computer code EPIC-2 gives extremely good simulations of the problem.

Approved for Public Release

---

**POSTAL ADDRESS:** Director, Materials Research Laboratories  
P.O. Box 50, Ascot Vale, Victoria 3032, Australia

---

SECURITY CLASSIFICATION OF THIS PAGE

UNCLASSIFIED

AD-0137 842

## DOCUMENT CONTROL DATA SHEET

REPORT NO.  
MRL-R-886AR NO.  
AR-003-299REPORT SECURITY CLASSIFICATION  
UNCLASSIFIED

## TITLE

BENDING OF BEAMS SUBJECTED TO TRANSVERSE IMPACTS

## AUTHOR(S)

R.L. WOODWARD

## CORPORATE AUTHOR

Materials Research Laboratories  
P.O. Box 50,  
Ascot Vale, Victoria 3032

## REPORT DATE

APRIL 1983

## TASK NO.

DST 82/103

## SPONSOR

DSTO

## CLASSIFICATION/LIMITATION REVIEW DATE

CLASSIFICATION/RELEASE AUTHORITY  
Superintendent, MRL  
Metallurgy Division

## SECONDARY DISTRIBUTION

Approved for Public Release

## ANNOUNCEMENT

Announcement of this report is unlimited

## KEYWORDS

Bending  
BeamsImpact  
Projectiles

## COSATI GROUPS

2011

## ABSTRACT

Transverse projectile impacts on the ends of free-free beams of circular cross section produced evidence of hinges in the beams and strain distributions which could be used for comparisons with a rigid-plastic approach to the dynamic response of structures and for comparisons with a finite element computer code solution. The rigid-plastic approach describes the mechanism of bending and hinge development and motion correctly but the simplifications inherent in the model prevent it from accurately predicting the detail. The computer code EPIC-2 gives extremely good simulations of the problem.

SECURITY CLASSIFICATION OF THIS PAGE

UNCLASSIFIED

# C O N T E N T S

	<u>Page No.</u>
1. INTRODUCTION	1
2. EXPERIMENT	1
3. RESULTS	2
4. DISCUSSION	3
5. CONCLUSION	7
6. ACKNOWLEDGEMENTS	8
7. REFERENCES	9

Accession For	
NTIS GRA&I	<input checked="" type="checkbox"/>
DTIC TAB	<input type="checkbox"/>
Unannounced	<input type="checkbox"/>
Justification	
By	
Distribution/	
Availability Codes	
Dist	Avail and/or Special
A-1	

# LIST OF SYMBOLS

$a, a_0, a_1$	=	linear acceleration	
$D$	=	beam diameter	
$l$	=	beam length	
$m$	=	mass per unit length	
$M_0$	=	limit moment of beam	
$M_x$	=	bending moment at position $x$	
$P$	=	load	
$V_x$	=	shear force at position $x$	
$x, x_h$	=	position, hinge position	
$Y$	=	yield stress of beam	
$\alpha, \alpha_0, \alpha_1$	=	angular acceleration	(Greek, L.C., Alpha)
$\Delta$	=	Mathematical Symbol - small change	(Greek, U.C., Delta)
$\epsilon$	=	Strain	(Greek, L.C., Epsilon)
$\theta$	=	angle	(Greek, L.C., Theta)
$\mu$	=	dimensionless load parameter	(Greek, L.C., Mu)
$\xi, \dot{\xi}$	=	dimensionless hinge position, rate of change of $\xi$	(Greek, L.C., Xi)
$\pi$	=	Constant	(Greek, L.C., Pi)
$\omega_0, \omega_1$	=	angular velocity	(Greek, L.C., Omega)

## BENDING OF BEAMS SUBJECTED TO TRANSVERSE

### IMPACTS

#### 1. INTRODUCTION

When a slender beam is subjected to a transverse impulsive force bending moments result due to the inertia of elements of the beam away from the site of loading. If the pulse is of sufficient magnitude then yielding or fracture may occur at the position of maximum bending moment. Zener and Peterson [1] demonstrated that when an impact occurs at the end of a freely suspended beam the point of maximum bending moment occurs at a distance one third of the beam length from the impact site. The problem of impact at the centre of free-free beams of either infinite [2] or finite [3] dimensions has been given more attention; under these conditions yielding occurs initially at the impact site about which two halves of the beam rotate. Symonds [4] and Symonds and Leth [5] examined how the detail of the loading and unloading cycle affects the nature and position of plastic hinges developed in centrally struck beams, and the influences of transverse shear and rotary inertia effects have been considered by Karunes and Onat [6] Symonds [7] and Jones and Gomes de Oliveira [8]. The main aspects of the theory have been reviewed in Johnson [9] and Goldsmith [10].

The present work concentrates on transverse impacts on one end of freely suspended beams, as it was found that under these conditions plastic hinges can be more easily produced away from the impact site than with central impacts. The work has direct relevance to the behaviour of slender rod shaped projectiles which break-up [1] or bend [11] at specific points along the length of the rod during impact. The results of experiments are compared with calculations based on the rigid-plastic theories described above, and with simulations using the finite element computer code EPIC-2 [12,13].

#### 2. EXPERIMENT

Beams of circular section were lightly glued to a support at one end and struck transversely with a projectile on the other end. The bond to the support was very weak so that the beams readily separated and were caught approximately 0.5 m away in a soft medium. The mild steel impactors were 4.76 mm diameter cylinders of mass 1.65 g, and on impact at  $775 \text{ m s}^{-1}$  they mushroomed, causing some local deformation to the end of the beam. The impact



conditions were estimated to be sufficient to exceed the shear yield stress on the beams. All post-impact measurements on the beams were taken from the centre of the impact site which was considered as the end of the beam for both the actual value of length to diameter ratio quoted and for the strain distributions.

The beams were circular in section, of diameter 6.35 mm, and of nominal length to diameter ratios 8, 12, 16 and 24. They were manufactured from a heat treatable steel (Vibrac R4) and used at various hardness levels from 355 HV10 to 575 HV10.

After impact the beam profile was projected onto a screen and traced, and the drawing divided into a series of segments along the length. Using the end of the beam away from impact to set a zero, the angle of the tangent to the beam was measured as a function of position along the beam on both the tension and compression sides. Assuming that the deformation is purely bending, the strain  $\epsilon$  in the outer fibres of a segment of beam of width  $\Delta l$  is given in terms of the diameter of the beam,  $D$ , and the change in tangent angle,  $\Delta\theta$ , across the segment by

$$\epsilon = \frac{D\Delta\theta}{2\Delta l} \quad (1)$$

The strain distribution as a function of position along the beam can thus be calculated. The results from compression and tension sides of the beam were similar, as expected for bending deformation, and hence only results from the tension side are reported.

### 3. RESULTS

Figure 1 shows the profiles of impacted beams of two strength levels and of various length to diameter ratios. In each beam except the shortest, in which it would be difficult to distinguish two bends because of their likely proximity, there are two major bends; one is approximately the same distance from the impact site in each beam regardless of strength or length to diameter ratio and the other is approximately half way along each beam. Fig. 2 shows results for beams all of length to diameter ratio approximately 11.2 but of a wide range of hardnesses. It is clear that the strength of the beams has influenced the amount of bending but not the position of the major hinges.

Strain distributions from the tension side of all beams in Fig. 1(a) and one from Fig. 2 are shown in Fig. 3 together with strain profiles from the computer simulations to be discussed.

#### 4. DISCUSSION

##### (a) Rigid-Plastic Approach

The development and motion of the hinges in impacted beams is readily described using the rigid plastic approach developed by Lee and Symonds [3] for central impacts on a free-free beam. In Lee and Symonds' case a beam of length  $2l$  is impacted in the centre, at which position a plastic hinge develops if the load is sufficient for the limit moment of the beam to be exceeded. To treat the end impact situation we use the same geometry but allow the centre of the beam to have a limit moment equal to zero; thus the beam yields at any load greater than zero and both rotates about the centre and accelerates in the direction of the impulse. It is then possible to focus on the right hand section of length  $l$  as a simulation of our end impact problem, the moment at both ends of one beam being zero and the first stage of the end impact problem corresponds to the second stage of the central impact problem of Lee and Symonds [3].

The situation is depicted in Fig. 4 where the impulsive force  $P$  is applied to a beam of length  $2l$ . At low impulsive forces each half of the beam will behave in a rigid manner with a linear acceleration  $a_0$  at the impact site and an angular acceleration  $\alpha_0$ , being positive clockwise for the right hand half which is to be considered. Using the same notation and method as Lee and Symonds [3]  $a_0$  and  $\alpha_0$  are given as

$$a_0 = 2P/ml \quad (2a)$$

$$\alpha_0 = 3P/ml^2 \quad (2b)$$

where  $m$  is the mass per unit length of the beam. The mean acceleration,  $a$ , of a length of beam distance  $x$  from the impact site and of mass  $(1-x)m$  is given by

$$a = a_0 - \frac{\alpha_0}{2} (x + 1) \quad (3)$$

Hence the shear force ( $V_x$ ) and bending moment ( $M_x$ ) at  $x$  are given by

$$V_x = m(1-x)a_0 + \frac{m}{2} (x^2 - 1^2) \alpha_0 \quad (4a)$$

$$M_x = \frac{m\alpha_0}{2} x^3 - \frac{m\alpha_0}{2} x^2 + ml \left( a_0 - \frac{\alpha_0}{2} \right) x + \frac{ml^2}{6} (2\alpha_0 l - 3a_0) \quad (4b)$$

Equating  $V_x$  to zero and substituting from (2) for  $a_0$  and  $\alpha_0$  shows that the maximum bending moment in the beam occurs where  $x = l/3$ , which is where initial yielding of the beam can be expected as  $P$  increased, and confirms the result of Zener and Peterson [1].

If the load is sufficient to exceed yield then there are two segments in the length  $l$  of the right half of the beam joined by a plastic hinge. The left segment has a linear acceleration  $a_0$  at the impact site and an angular acceleration  $\alpha_0$ , and the right hand segment has a linear acceleration  $a_1$  at the end of the beam and an angular acceleration  $\alpha_1$ . Corresponding angular velocities in the sections are  $\omega_0$  and  $\omega_1$ . The load is expressed in terms of the limit moment,  $M_0$ , of the beam using the parameter  $\mu$ ,

$$\mu = \frac{Pl}{M_0} \quad (5)$$

The position of the hinge,  $x_h$ , is given dimensionlessly as  $\xi$  by

$$\xi = x_h/l \quad (6)$$

where  $\xi$  may be finite. The equations of motion of the two segments become

$$\frac{a_0}{l} = \frac{M_0}{ml^3} \left( \frac{2\mu}{\xi} - \frac{6}{\xi^2} \right) \quad (7a)$$

$$\alpha_0 = \frac{M_0}{ml^3} \left( \frac{3\mu}{\xi^2} - \frac{12}{\xi^3} \right) \quad (7b)$$

$$\frac{a_1}{l} = -\frac{M_0}{ml^3} \frac{6}{(1-\xi)^2} \quad (7c)$$

$$\alpha_1 = \frac{M_0}{ml^3} \frac{12}{(1-\xi)^3} \quad (7d)$$

$$\frac{M_0}{ml^3} \left[ \frac{\mu}{\xi} - \frac{6}{\xi^2} + \frac{6}{(1-\xi)^2} \right] = -\dot{\xi} (\omega_0 - \omega_1) \quad (7e)$$

These equations are only slight modifications of the equations given by Lee and Symonds [3] for the central impact problem. With equations (5), (6) and (7) and the velocity and acceleration formulas established by Lee and Symonds [3] it is possible to calculate numerically the positions of hinges and the profile of a beam as a function of time for the loading function  $P$ . In

comparing the calculations with end impact experiments it is noted that  $P$  is obtained by doubling the load applied to the end of a single beam in the experiment.

Numerical evaluation of the equations shows that the beam rotates as a rigid body as the load increases until a hinge develops one third rod length from the impact site. With further increase in load the position of the hinge moves either towards the impact site for slender beams or towards the centre for beams of low length to diameter ratio. If the load  $P$  is sufficient to cause shear yielding of the end of the beam then a limit is reached [6,7,8] because shear sliding occurs on the end at constant stress. In this case the beam is effectively subjected to a constant end load and the hinge becomes stationary. If the load decreases to zero the plastic hinge moves towards the beam centre, the beam continuing to bend as the hinge moves until the angular velocities on either side of the hinge become equal at the time the hinge reaches the centre.

For a circular beam the load,  $P$ , at which the shear yield stress is exceeded is given by

$$\frac{P}{2} = \frac{\pi}{4\sqrt{3}} Y D^2 \quad (8)$$

The limit moment,  $M_0$  for a circular beam is

$$M_0 = 1/6 Y D^3 \quad (9)$$

Substituting (8) and (9) in (5) and putting  $\omega_0 = \omega_1$  and evaluating equation (7e) gives the hinge position as a function of length to diameter ratio of the beam, as shown in Fig 5. At times greater than zero,  $\omega_0 > \omega_1$  necessarily and if the load exceeds the shear yield stress  $P$  will continue to be given by equation (8), hence  $\mu$  is constant and the sign of  $\xi$  can be evaluated using equation (7e) for hinge positions to either side of the initial value. The sign of  $\xi$  is such as to return the hinge to its initial position, hence whilst  $\mu$  remains constant, bending will continue about the initial hinge position. The bending moment at yield of the outer fibres is  $3\pi/16$  times the limit moment given by equation (9) and hinge positions evaluated using this yield moment are also given in Fig 5. For long length to diameter ratio beams Fig 5 shows the hinge positions approach limits in terms of beam diameter whichever moment value is used. The value approached for the limit moment case, equation (9), is approximately 1.1 beam diameters, and this agrees with the value found by adapting Symonds [7] later work on beams of infinite length.

The major hinge near the impact site was observed to be in an approximately constant position independent of the beam strength or length to diameter ratio, Figs. 1 and 2, which is expected, based on the above reasoning for the situation in which the shear yield stress is exceeded, and for the length to diameter ratios used. However, the hinge position in all cases is between two and four beam diameters from the centre of impact: the average is

very close to three. This is much larger than the 1.1 diameters expected using the limit moment in the theory described above and the departure is still greater if the yield moment is considered, Fig. 5. Quasi-static four point bend tests on some of the beams showed that for these beams and angles of bend the yield moment was a better estimate of the bend strength. If the inner edge of the impact site is used instead of the centre of impact then there is a slight improvement but still the major hinge is too far from the end of the beam. The model has a limitation in that it requires bending to occur at a point whereas in practice one would expect the width of the hinge to be at least of the order of the beam diameter, which is the order of the prediction of hinge distance from the impact site.

Estimates of projectile contact time from computer simulations (below) were between 20 and 30 microseconds. Yield stresses for equations (8) and (9) were estimated as 2.9 times the Vickers hardness of the beams. Allowing a constant load, exceeding the shear yield stress, at the end of the beam for these contact times gave bend angles which were too large but the deflection of the impact point was predicted to well within the correct order of magnitude and also varied in the correct manner with length to diameter ratio using the rigid plastic approach. More precise calculations would require an exact knowledge of the loading history.

#### (b) Computer Simulation

Computer simulation offers the opportunity to study the detailed development of the hinges with time and at the same time the loading can be readily handled. The computer code used was EPIC-2 which is a finite element code in two dimensions. Thus the simulation is in plane strain although the event being simulated is three dimensional and exact agreement should not be anticipated. Most simulations used eight triangular elements across the beam depth, although one problem was also run with twelve elements across to determine whether grid refinement had any significant effect. Failure strains for the beam were made large so that only plastic flow was allowed, no fracture having been observed in experiments.

The effective strains in surface elements are plotted in Fig. 3 for comparison with experimental measurements. The magnitudes of the strains agree well with the experimental results except for the case of Fig. 3(a), and as noted previously in reference to Fig. 1(a), the strains in this beam were unusually low. The maxima in the strain distributions from the simulation are in approximately the correct position and in changing from a soft to a hard beam at the same length to diameter ratio the main peak is observed to broaden and its magnitude to decrease in both the experiment and the simulation, Figs. 3(c) and (e). The simulation gives two distinct peaks in strain, one near the impact site and one near the centre of the beam, and some minor peaks between these. The mean position of the major hinge from the code solutions was 2.5 diameters from the impact site for those cases simulated. The actual position varied slightly with the length to diameter ratio and strength of the beam but whether or not this is a true variation is not evident from the solutions as the uncertainty due to grid size, ( $\pm$  one quarter beam diameter), is of the order of the variation in position. The use of a finer grid size only slightly modifies the observed strain distribution, Fig. 3(c). As can be

expected from the description of the strain distributions, the final profiles from the computer simulation were very close to those observed in experiments.

A plot of a typical strain distribution across a beam is shown in Fig. 6(a). Adjacent to the impact site the plastic strain contours go almost straight across the beam which confirms the estimate that the loading was sufficient to cause shear yielding of the end of the beam. Further along the beam the symmetrical nature of the strain profile confirms that the problem is essentially one of simple bending as described in the Lee and Symonds [3] model. The development of the strain in the outer fibres as a function of time is shown in Fig. 6(b). The rise in strain towards the impact site is associated with localized impact damage. Up to 30 microseconds, during which time the load is applied, a peak develops around one point in the beam although the effect of a finite width is evident as the peak is broad. After 30 microseconds the projectile had left the beam but plastic bending continues to occur because of the momentum of the beam, and the hinge moves towards the beam centre, as described above using the rigid plastic model. When the hinge reaches the centre bending continues and develops another large strain peak, contrary to what was expected from the rigid-plastic model. The velocity profiles at 30, 50, 70 and 100 microseconds are shown in Figs. 6(c) to (f) for the case shown. At 30 microseconds the situation is far from the idealization of two rigid sections bending about a hinge. At this stage, however the major hinge is the only place at which significant plastic deformation is occurring. Whilst the load has been removed at 50 microseconds the velocity distribution is still very complex and at 70 microseconds a comparison of velocity vectors at equal distances either side of the point of rotation shows that bending continues to occur. At 100 microseconds the beam is essentially rotating.

It is clear from these velocity profiles that although most plastic strain is associated with the type of deformation described in the simple rigid-plastic model, both during loading and as the hinge moves to the centre after load removal, in the experimental situation neither segment of the beam is near stress equilibrium at any stage. If the impact site is still moving too fast and the distal end of the beam too slowly when the hinge reaches the centre, then each half of the beam can be elastically bent to the yield stress. Locally, the bending may cease instantaneously as the hinge reaches the centre but the elastic bending in the two halves of the beam will then add to exceed the yield stress causing further strain at the centre. The relief of elastic bending of the segments then provides a possible explanation of the strain peak near the centre of the beams.

## 5. CONCLUSION

Dynamic impact experiments were carried out on the end of free-free beams of circular section and the positions of hinges and the overall strain distributions compared with rigid-plastic model and computer code predictions. The basic deformation mechanism described by the model is confirmed, but it predicts a hinge position too close to the impact site because it does not take account of the finite width of the hinge. In the experiments a further major bend was observed near the centre of the beams, probably associated with the relief of elastic stress in the two segments of

the beam, a factor which also can not be included in the rigid plastic model. The rigid-plastic model provides a clear explanation for the development of a stationary hinge whilst the beam is loaded and for the movement of the hinge when the load is removed. The use of a finite element computer code allowed the loading cycle on the beam to be simulated, giving extremely good agreement with the experimental strain distributions, confirming the nature of the deformation as essentially a bending process.

#### 6. ACKNOWLEDGEMENTS

The computer code EPIC-2 was provided by the US Army ARRADCOM Ballistic Research Laboratory and the author is grateful for the assistance of Dr J.A. Zukas, G.H. Jonas, J. Missey and Mrs B. Ringers in his introduction to the method. The assistance of Mr N.J. Baldwin with some of the experimental work is gratefully appreciated.

## 7. REFERENCES

1. Zener, C. and Peterson, R.E. "Mechanism of Armour Penetration". Second partial report, No. 710/492 Watertown Arsenal, Mass., 1943.
2. Hopkins, H.G., "On the Behaviour of Infinitely Long Rigid-Plastic Beams Under Transverse Concentrated Load". J. Mech. Phys. Sol., Vol. 4, 1955, pp. 38-52.
3. Lee, E.H. and Symonds, P.S., "Large Plastic Deformations of Beams Under Transverse Impact". Trans. A.S.M.E., J. Appl. Mechs., Vol. 74, 1952, pp.308-314.
4. Symonds, P.S., "Dynamic Load Characteristics in Plastic Bending of Beams". Trans. A.S.M.E., J. Appl. Mechs., Vol. 20, 1953, pp. 475-481.
5. Symonds, P.S. and Leth, C.F.A., "Impact of Finite Beams of Ductile Metal". J. Mech. Phys. Sol., Vol. 2, 1954, pp. 92-102.
6. Karunes, B. and Onat, E.T., "On the Effect of Shear on Plastic Deformation of Beams Under Transverse Impact Loading". Trans. A.S.M.E., J. Appl. Mechs., Vol. 27, 1960, pp. 107-110.
7. Symonds, P.S., "Plastic Shear Deformation in Dynamic Load Problems", Engineering Plasticity, Ed. J. Heyman and F.A. Leckie, C.U.P. London, 1968, pp. 647-664.
8. Jones, N. and Gomes de Oliveira, J., "The Influence of Rotary Inertia and Transverse Shear on the Dynamic Plastic Behaviour of Beams". Trans. A.S.M.E., J. Appl. Mechs., Vol. 46, 1979, pp. 303-310.
9. Johnson, W., "Impact Strength of Materials", Arnold, London, 1972, pp. 250-280.
10. Goldsmith, W., "Impact", Arnold, London, 1960, pp. 206-233.
11. Reid, S.R., Edmunds, A.J. and Johnson, W., "Bending of Long Steel and Aluminium Rods During End Impact with a Rigid Target". J. Mech. Engng. Sci., Vol. 23, 1981, pp. 85-92.
12. Johnson, G.R., "EPIC-2, A Computer Program for Elastic-Plastic Impact Computations in 2 Dimensions Plus Spin". US Army ARRADCOM Ballistic Research Laboratory Contract Report ARBRL-CR-00373, June, 1978.
13. Johnson, G.R. "Analysis of Elastic-Plastic Impact Involving Severe Distortions". Trans. A.S.M.E., J. Appl. Mechs., Vol. 43, 1976, pp. 439-444.





(a)



(b)

FIG. 1 (a) Profiles of beams of hardness 395HV10 and length to diameter ratios 23.8, 15.3, 11.6 and 7.3.  
(b) Profiles of beams of hardness 480HV10 and length to diameter ratios 23.5, 15.6, 11.4 and 7.4.

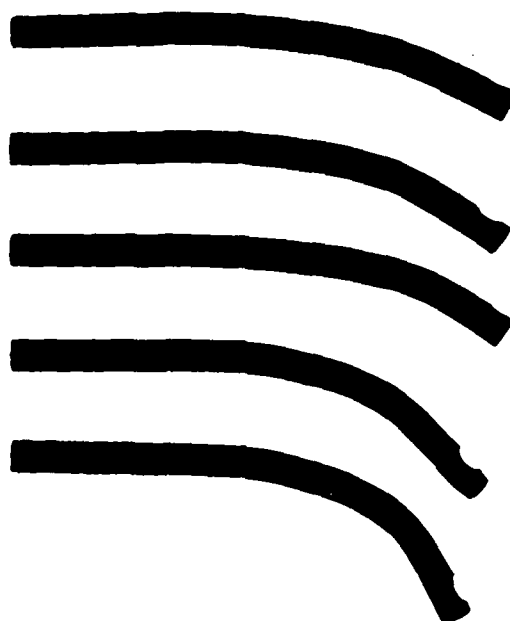


FIG. 2 Beams of length to diameter ratio approximately 11.2 and of hardnesses, top to bottom, 575HV10, 480HV10, 450HV10, 395HV10 and 355HV10.

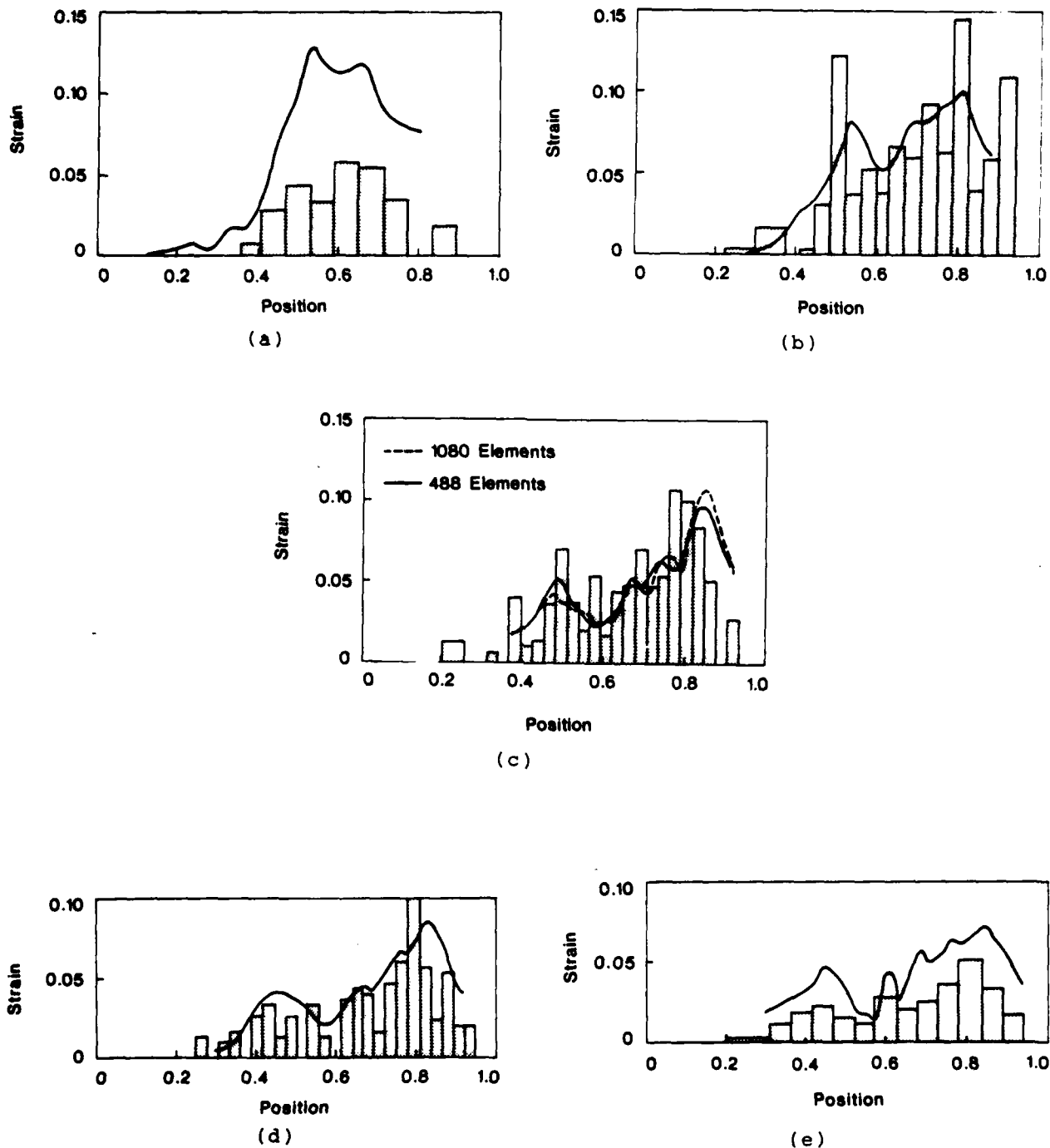


FIG. 3 Strain distributions for the tension side of beams of hardness 395HV10 and of length of diameter ratios (a) 7.3, (b) 11.6, (c) 15.3 and (d) 23.8 from Fig. 1(a), and (e) of length to diameter ratio 11.2 and hardness 575HV10 from Fig. 2. In each case the histogram represents experimental measurements from the bent beams and the continuous line the results of simulations using the EPIC-2 computer program. Computer simulations were done with two grid sizes for case (c).

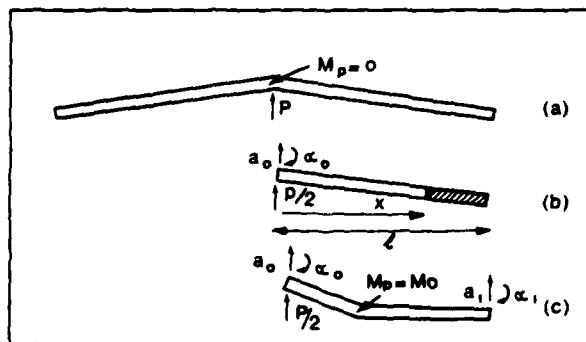


FIG. 4 (a) Impulsive force  $P$  applied to a beam of length  $2l$  as in Lee and Symonds [3] but the limit moment,  $M_p$ , is set to zero at the central hinge so that the beam bends for any finite load.

(b) Motion of rigid beam of length  $l$  at loads below that sufficient to cause yielding. The load  $P/2$  applies to the beam length  $l$  which experiences a linear acceleration  $a_0$  at the impact site and an angular acceleration  $\alpha_0$ .

(c) At loads sufficient for the limit movement  $M_p$  to be exceeded, two rigid segments are joined by a plastic hinge the limit moment being given by  $M_0$  in equation (9). The linear accelerations of the impact and distal ends are  $a_0$  and  $a_1$  respectively and the angular accelerations of the corresponding segments are  $\alpha_0$  and  $\alpha_1$ .

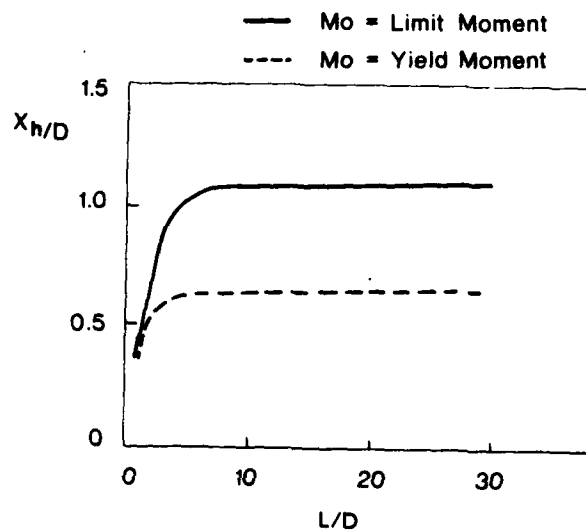
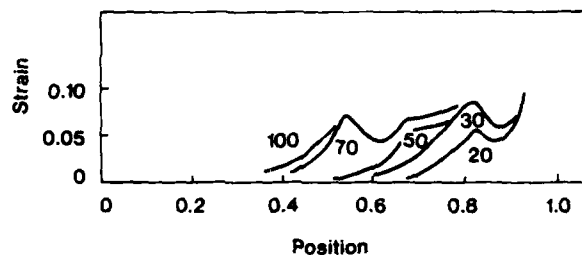


FIG. 5 Hinge position divided by beam diameter ( $x_h/D$ ) as a function of length to diameter ratio ( $L/D$ ) for the case where shear yielding occurs at the impact site. Two situations are shown, in one case the beam bends plastically at the limit moment (Equation (9)) and in the other it bends plastically at the yield moment.



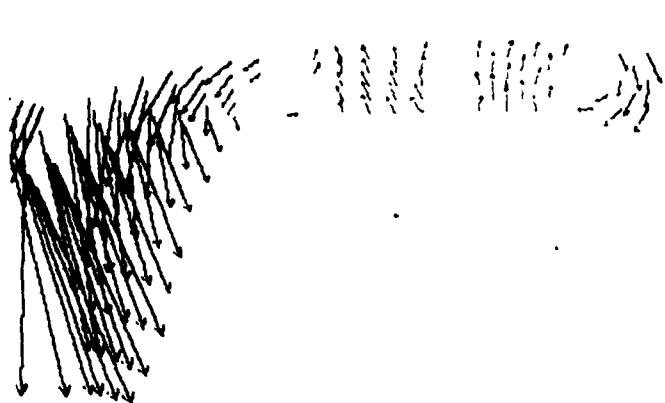
(a)



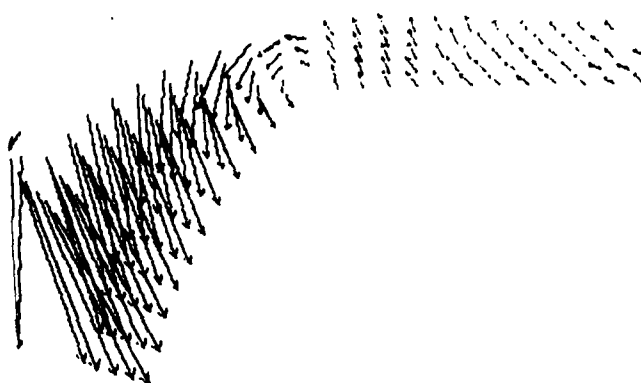
(b)

FIG. 6 (a) Strain distribution from the computer simulation in a beam of length to diameter ratio 11.6 and of the same strength as the beams of Fig. 1 (a). The strain contours have values of natural strain 0.01, 0.02, 0.04, 0.06 and 0.07 and the strain increases on moving out from the neutral axis of the beam.

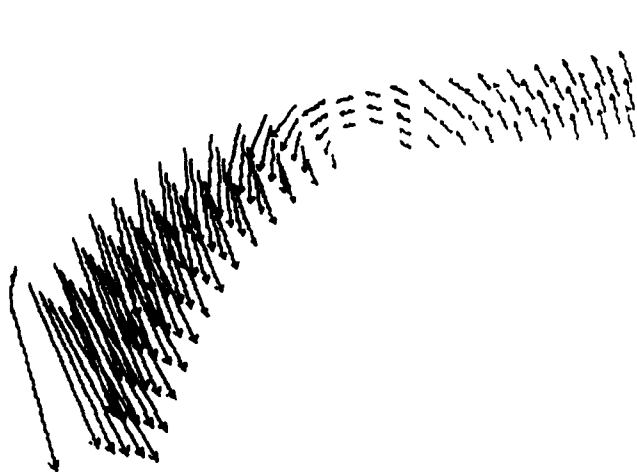
(b) Values of effective strain at the surface as a function of fractional position along the beam for the same problem as above at the times indicated on the curves, in microseconds. Only that part of the curve which has changed with increase in time is shown.



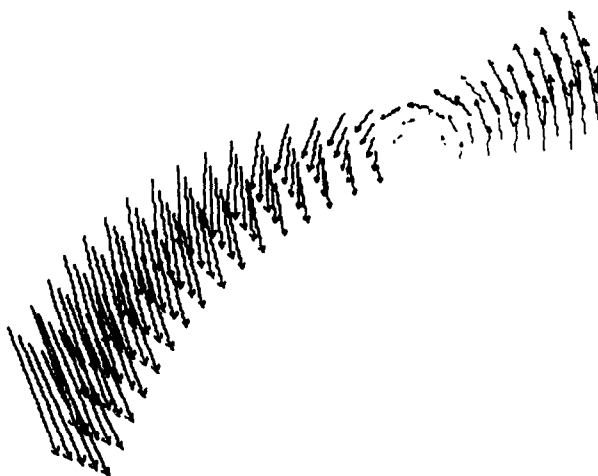
(c)



(d)



(e)



(f)

FIG. 6 (c) to (f) Velocity vectors along the beam for the case shown above at times (c) 30 microseconds, (d) 50 microseconds, (e) 70 micro-seconds and (f) 100 microseconds.

DISTRIBUTION LIST

MATERIALS RESEARCH LABORATORIES

Director  
Superintendent, Metallurgy Division  
Dr C.W. Weaver  
Library (2 copies)  
Dr R.L. Woodward

DEPARTMENT OF DEFENCE

Chief Defence Scientist/Deputy Chief Defence Scientist/ (1 copy)  
Controller, Projects and Analytical Studies/  
Superintendent, Science and Technology Programme  
Controller Services Laboratories and Trials  
Army Scientific Adviser  
Air Force Scientific Adviser  
Navy Scientific Adviser  
Officer-in-Charge, Document Exchange Centre (17 copies)  
Technical Reports Centre, Defence Central Library  
Central Office, Directorate of Quality Assurance - Air Force  
Deputy Director Scientific and Technical Intelligence,  
Joint Intelligence Organisation  
Librarian, Bridges Library  
Librarian, Engineering Development Establishment  
Defence Science Representative, Australia High  
Commission, London (Summary Sheets Only)  
Counsellor Defence Science, Washington, D.C. (Summary Sheets Only)  
Librarian, (Through: Officer-in-Charge), Materials Testing  
Laboratories, Alexandria, NSW  
Senior Librarian, Aeronautical Research Laboratories  
Senior Librarian, Defence Research Centre, Salisbury, SA  
Director, Weapons Systems Research Laboratory  
Director, Electronics Research Laboratory  
Director, Advanced Engineering Laboratory  
Superintendent, Trials Resources Laboratory  
Librarian, RAN Research Laboratory

DEPARTMENT OF DEFENCE SUPPORT

Deputy Secretary, DDS  
Director Industry Development, Melbourne, Vic.  
Head of Staff, British Defence Research & Supply Staff (Aust.)  
Controller, Munitions Supply Division  
Controller, Aircraft, Guided Weapons & Electronics Supply Division  
Manager, Ordnance Factory, Bendigo, Vic.  
Manager, Ordnance Factory, Ascot Vale, Vic.  
Manager, Ammunition Factory, Footscray, Vic.  
Manager, Small Arms Factory, Lithgow, NSW  
Manager, Government Aircraft Factory, Port Melbourne, Vic.



DISTRIBUTION LIST  
(Continued)

OTHER FEDERAL AND STATE DEPARTMENTS AND INSTRUMENTALITIES

NASA Canberra Office, Woden, ACT  
The Chief Librarian, Central Library, CSIRO  
Library, Australian Atomic Energy Commission Research Establishment  
Librarian, National Measurement Laboratory  
Chief, Division of Tribophysics, CSIRO  
Chief, Division of Mechanical Engineering, CSIRO  
Chief, Production Technology Laboratory, Division of Materials  
Science, CSIRO  
General Manager, Commonwealth Aircraft Corporation

MISCELLANEOUS - AUSTRALIA

Deputy Registrar, National Association of Testing Authorities  
Assistant Technical Director, Standards Association of Australia  
Librarian, State Library of NSW, Sydney, NSW  
University of Tasmania, Morris-Miller Lib., Hobart, Tas.

MISCELLANEOUS

Assistant Director/Armour and Materials, Chertsey, England  
Reports Centre, Directorate of Materials Aviation, England  
Library - Exchange Desk, National Bureau of Standards, USA  
UK/USA/CAN/NZ ABCA Armies Standardisation Representative (4 copies)  
The Director, Defence Scientific Information & Documentation  
Centre, India  
Military, Naval and Air Adviser, High Commission of India, Canberra  
Director, Defence Research Centre, Kuala Lumpur, Malaysia  
Exchange Section, British Library, UK  
Periodicals Recording Section, Science Reference Library,  
British Library, UK  
Library, Chemical Abstracts Service  
INSPEC: Acquisition Section, Institute of Electrical Engineers, UK  
Engineering Societies Library, USA  
Director, Admiralty Materials Laboratory, UK  
Director, Propellants, Explosives & Rocket Motor Establishment, UK  
Director, Royal Aircraft Establishment, UK  
Director, Royal Armament Research & Development Establishment, UK  
Aeromedical Library, Brooks Air Force Base, Texas, USA  
Ann Germany Documents Librarian, The Centre for Research  
Libraries, Chicago Ill.  
Defense Attache, Australian Embassy, Bangkok, Thailand  
(Att. D. Pender)

(MRL-R-886)

DISTRIBUTION LIST  
(Continued)

ADDITIONAL DISTRIBUTION

US Army ARRADCOM Ballistics Research Laboratory  
(Att. Dr J. Zukas, Mrs B. Ringers)  
Dr Gordon R. Johnson, Honeywell Inc.

(2 copies)

